Deep-well, Low-flow Photovoltaic Water Pumping System Design

University of California, San Diego
Jacobs School of Engineering
Department of Mechanical and Aerospace Engineering
MAE 199 – Dr. Jan Kleissl

Anders Nottrott

Abstract

This report presents a proposed design for a deep-well, photovoltaic water pumping system to be installed at the Puma Canyon Ranch in Goleta, California. The proposed design is intended to replace the existing system that pumps water from the New West well using energy supplied by the public power grid. This paper discusses methods for determining the available solar energy at a particular geographic location, methods for designing piping systems and the general components required to build a functional photovoltaic water pumping system. Based on the cost analysis of the proposed design it is determined that deep-well, low-flow photovoltaic water pumping systems are not a viable solution for supplying water to small scale agricultural applications. However, these systems have several characteristics that make them an innovative solution for supplying water in other applications.

Introduction

The increasing costs of energy and the desire for environmentally sustainable solutions to existing engineering challenges necessitate the application of alternative energy sources to modern engineering systems. In this context an alternative energy source is defined as a continually renewable mechanism for generating electrical power that does not require the combustion fossil fuels, or significantly affect the natural environment by its mode operation. In addition to the increased demand for renewable energy there is also a continual demand for fresh water to sustain settlement and agricultural enterprises. When a fresh water source is located a long distance from a desired delivery site, the source lies deep below ground or the available source produces water at insufficient pressures, conventional energy derived from fossil fuels is often used to pump the water to a more useful location. The goal of this report is to present a comprehensive case study of the methods for the design of photovoltaic water pumping systems by developing a site specific deep-well pumping system powered entirely by solar energy.

This report provides a detailed design analysis for a deep-well, low-flow photovoltaic water pumping system that will be installed in the New West well at the Puma Canyon Ranch in Goleta, California. The Puma Canyon Ranch is a privately owned organic avocado farm that is operated in cooperation with the Growing Solutions Restoration Education Institute. The motivation for the design is to help improve the environmental sustainability of ranch operations and reduce the dependence on electricity drawn from the main power grid. The system pumps water from the well to an elevated storage tank with sufficient altitude to supply water for agricultural and domestic use. The overall design is based on the criteria that the system must be simple to operate, functional without an the presence of an operator, require minimal inspection and maintenance once established, use the smallest amount of energy possible and have a projected service lifetime of at least 15 years.

Energy Analysis

Photovoltaic arrays are reliable power supplies with highly variable outputs. Generally the power output of a photovoltaic array depends on the amount of solar irradiance it receives and the operating temperature of the array. The larger the amount of solar irradiation an array receives the greater its power output.[1,2] The power output of an individual photovoltaic module also depends on its operating temperature, and a broad trend shows that as the Nominal Operating Cell Temperature (NOCT) increases the power output of the module decreases.[3] These trends illustrate that the power output of individual photovoltaic modules and the total energy available form photovoltaic arrays is highly dependent on the environment in which they are installed. This fact underscores the need for a thorough, site specific solar irradiance analysis that should be performed as a first step in the design process in order to make a realistic estimate for how much power will be available from a photovoltaic array installed in a particular geographic location.

Theoretical Solar Irradiation Modeling

Preliminary estimates for the amount of solar irradiation available at any particular geographic location are best determined using theoretical modeling techniques. The solar power density at the top of the Earth's atmosphere is given by the solar constant whose value is $1367 W/m^2$.[4] The amount of solar radiation that reaches the Earth's surface from outer space is significantly reduced by diffusion and scattering in the Earth's atmosphere. Meinel and Meinel[5] determined that the relationship between the solar irradiance at the surface of the Earth and the air mass through with the radiation must pass is given by,

$$I = 1367(0.7)^{AM^{0.678}} \qquad (1)$$

The air mass (AM) refers to the optical length that light from an extraterrestrial source must travel to reach Earth's surface. The air mass is a function of the reference air mass distance (AM_{ref}) and the solar altitude angle (α)[6],

$$AM = AM_{ref}(\csc\alpha) \quad (2)$$

The reference air mass distance is defined as the air mass distance at solar noon when the sun is directly overhead, and is generally taken as $AM_{ref} = 2$.[7] In this analysis a conservative reference value of $AM_{ref} = 2.5$ has been used in order to avoid overestimating the amount of available solar energy. The solar altitude angle represents the angle between the horizon and the incident solar beam and is a function of latitude (φ), the solar declination (δ) and the hour angle (ω),[8]

$$\alpha = \arcsin\left(\sin\delta\sin\varphi + \cos\delta\cos\varphi\cos\omega\right) \qquad (3)$$

The latitude for the site selected for solar array installation was determined using a Garmin GPS 76 Global Position System (GPS) and is taken as $\varphi = 34.47663^{\circ}$. The solar

declination angle represents the angle that the sun deviates from the line perpendicular to the Earth's equator and it varies throughout the year with[9],

$$\delta = 23.45° \sin\left(\frac{360(n-80)}{356}\right) \quad (4)$$

The value of *n* in Equation 4 represents the day of the year, and *n* takes integer values in the set [1,365]. The hour angle is the angle between the sun's position at noon and its position at any given time of the day. This relationship is given by[10],

$$\omega = 15(12 - T)° \quad (5)$$

In Equation 5 *T* is the time of day on 24-hour scale. The sunrise and sunset angle for a particular latitude is defined in terms of the hour angle and is a function of the solar declination angle[11].

$$\omega_{rise,set} = \pm \arccos(-\tan\varphi \tan\delta) \quad (6)$$

By combining Equations 4,5 and 6 and performing algebraic manipulations an approximate formula for the sunrise and sunset time for a particular latitude on any given day of the year is easily obtained. The result yields,

$$T_{rise,set}(n) = 12 \pm \left(\frac{1}{15}\right) \arccos\left\{-\tan\varphi \tan\left[23.45 \sin\left(\frac{360(n-80)}{365}\right)\right]\right\} \quad (7)$$

$$where,\ n \in Z = [1,365]$$

Using these equations, a value for the total solar energy density available on Earth's surface, after the effects of atmospheric diffusion and scattering, can be obtained for a particular latitude on any given day of the year. Equations 1,2,3,4 and 5 may be combined and integrated over the whole day to yield the total theoretical solar energy density as a function of the day of the year in units of $kW{\cdot}h/m^2$.

$$P(n) = 1.367 \int_{T_{rise}}^{T_{set}} 0.7^{AM_{ref}\left\{\csc\left[\arcsin\left(\sin\left(\frac{72(n-80)}{73}\right)\sin\varphi + \cos\left(\frac{72(n-80)}{73}\right)\cos\varphi\cos(15(12-T))\right)\right]\right\}} dT \quad (8)$$

$$where,\ n \in Z = [1,365]$$

Equation 8 provides a complex analytical relationship for theoretical solar energy density, which is readily resolved with the help of numerical computation tools. In this analysis MATLAB was used to compute the sunset and sunrise time for each day of the year using Equation 7 and then to numerically integrate Equation 8 for P(n) on each day of the year.

Figure 1 is a plot of P(n) for one calendar year. It is important to understand that this method for computing the daily solar energy density yields only theoretical results. Because Equation 8 does not account for atmospheric effects like humidity, cloud cover,

air temperature and composition variations and the presence of solid particles in the atmosphere, the theoretical values of P(n) are significantly higher than measured experimental values. Never the less Equation 8 provides a good preliminary estimate for

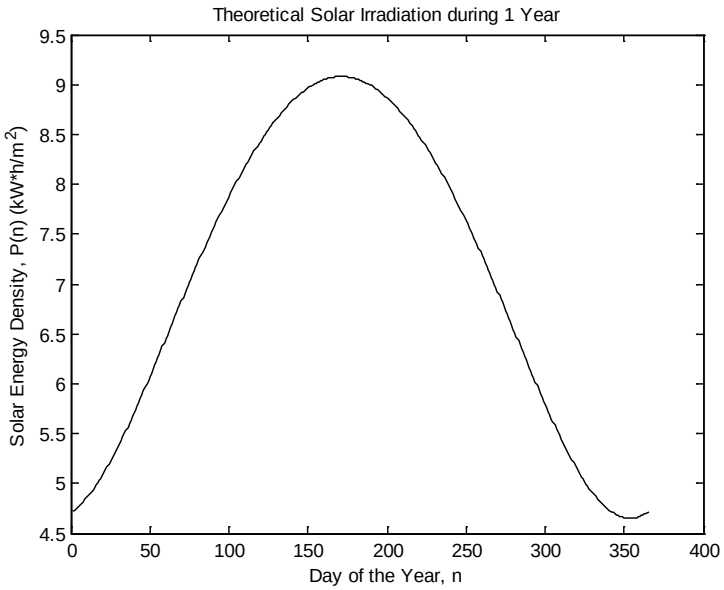

Fig. 1 Theoretical solar irradiation during one year at the Puma Canyon Ranch in Goleta, California

the available solar energy density at a specific geographical location and is particularly useful when no experimental solar irradiance data exist for a proposed solar energy collection site. When experimental solar energy data is available, however, both methods should be employed for modeling solar energy and subsequent design of photovoltaic powered systems should be based largely on the experimental results rather than the theoretical results.

Modeling Solar Irradiance and Irradiation from Experimental Data

A solar irradiance or irradiation model that is developed from experimental data collected at or near a prospective solar collection site provides the most accurate method for estimating the output of solar arrays installed at that location. The California State Department of Water Resources (DWR), Office of Water Use Efficiency maintains a program called the California Irrigation Management Information System (CIMIS), which provides a large volume of atmospheric data collected at various weather stations throughout the state. The DWR maintains several CIMIS weather stations in Santa Barbara County and the nearest station to the Puma Canyon Ranch is the Goleta Foothills Station #94,[12] which is approximately 3.2 kilometers ESE of the proposed location for constructing the solar arrays, lies at an elevation of 195 meters, and 30 meters above the proposed location for the solar collector.[*] The station has been in nearly continuous operation since July 1990 and collects data on daily solar energy density using a Global

[*] The approximate distance and altitude change between the CIMIS Station #94 and the prospective site for the solar collector, was determined using the U.S. Department of the Interior, U.S. Geological Survey maps of Dos Pueblos Canyon, CA and Goleta, CA.

Solar Radiation Pyranometer model number LI200S and manufactured by Li-Cor.[13] Data collected from this station are publicly available on the CIMIS website and on the website for the California Climate Data Archive (CalClim), a joint project between the

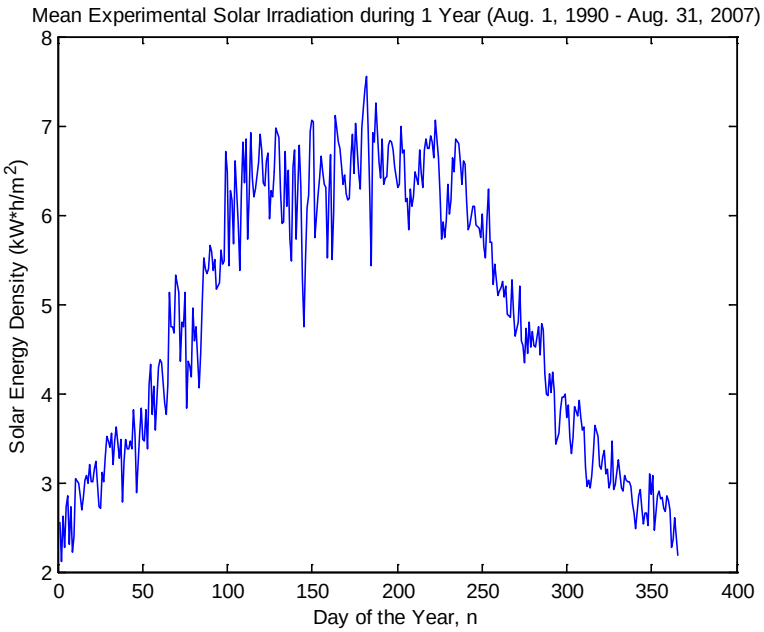

Fig. 2 Experimental solar irradiation during one year at the CIMIS Station #94 in Goleta, California

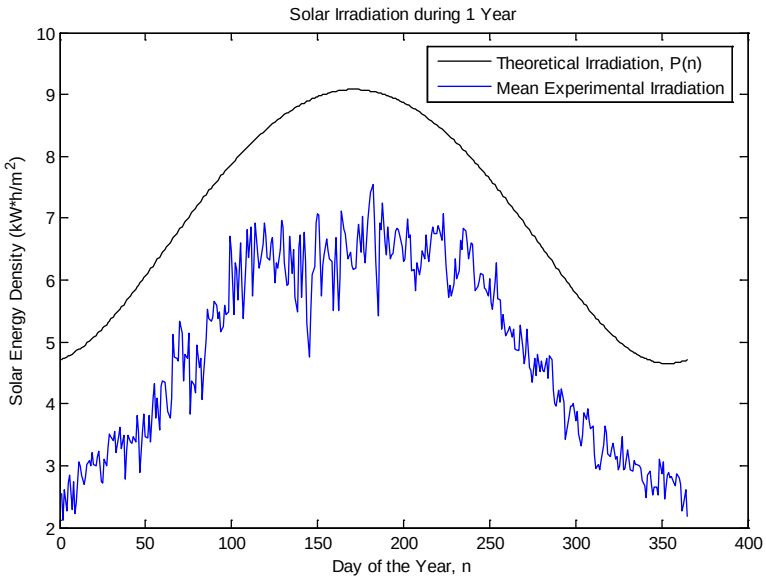

Fig. 3 Theoretical solar irradiation data plotted with experimental irradiation data for 1 year

Western Regional Climate Center, Scripps Institution of Oceanography and the California Energy Commission.[14] This analysis used data from the CalClim website because of the convenient formatting of the raw data set. The analysis was for daily solar

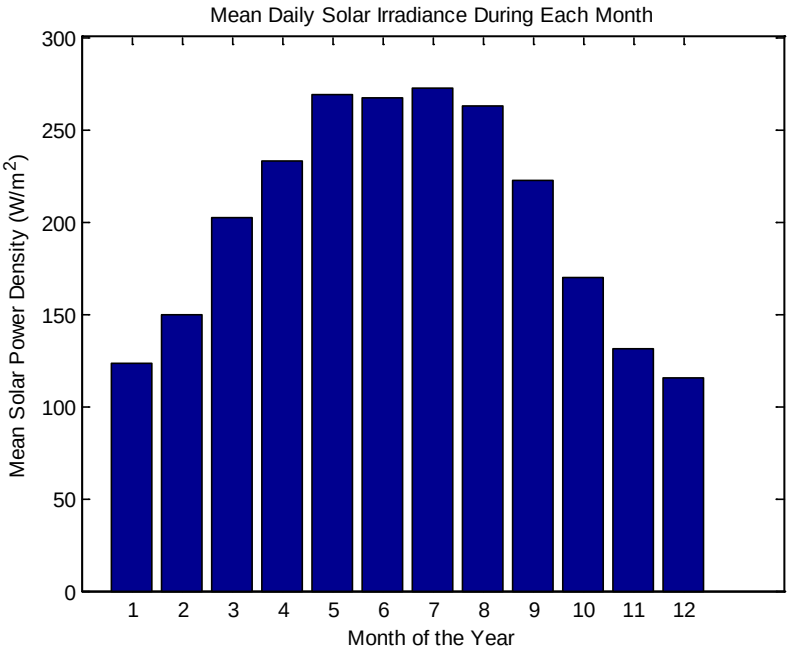

Fig. 4 Mean experimental daily solar power density by month at the CIMIS Station #94 in Goleta, California

irradiation data collected during a period beginning on August 1, 1990 and ending on August 31, 2007, and for monthly solar irradiance data collected during a period beginning in July 1990 and ending in April 2007. The solar irradiation data consists of total daily irradiation values measured by the pyranometer for each day of the year during the experimental period. In order to determine a nominal value for total daily solar irradiation on each day of the year, the yearly values for total daily irradiation were averaged for each day of the year. The results are shown in Figure 2. This plot of the experimental data can be used to assess the validity of the theoretical model for daily solar energy density by plotting them on the same graph. Figure 3 shows that while the theoretical model follows the same general trend as the experimental data, the values predicted by the theoretical model are significantly greater than those indicated by the experimental data.

Month	Mean Peak Sun Hours (Hours/Day)
January	3.0
February	3.6
March	4.9
April	5.6
May	6.5
June	6.4
July	6.5
August	6.3
September	5.3
October	4.0
November	3.2
December	2.8

Table 1 Peak Sun Hours per day during each month at the Puma Canyon Ranch

The data from the CalClim website was also used to compute the mean daily solar power density during each month of the year and the mean number of peak sun hours per day during each month. In the solar irradiance data set monthly average values for total solar power density were averaged for each month during the experimental period, and these monthly values were divided by the number of days in each month to determine the mean daily solar power density. These values are shown in Figure 4. The number of peak sun hours is defined as the

number of hours at an irradiance level of 1 kW/m^2 required to produce the total solar energy density available in 1 day.[15] Peak sun hours are determined from the monthly mean solar irradiance values and are an indicator of how many hours per day solar arrays will operate at peak power output. Mean daily peak sun hours during each month are shown in Table 1. When the power requirements of the pumping system have been determined, peak sun hours can also be used to estimate the amount of water that will be pumped by the system.

Mechanical Design

The number and type of individual solar modules that will be used to power the water pumping system is dependant on the power requirements of the system's mechanical components. Before the proper solar modules can be selected it is necessary to develop an engineering model that defines the essential parameters of the system so that the mechanical components can be selected. The selection of piping materials and pumps is based on the mechanical constraints imposed on the system by the engineering model, goals for improvement over the existing pumping system and the goal of long-term reliability of the system with minimal maintenance.

The Engineering Model

The engineering model that defines the mechanical parameters of the solar powered water pumping system at the Puma Canyon Ranch is based on data collected by current and previous ranch owners, data and measurements obtained from the original well driller and physical measurements made by the authors during a comprehensive survey performed at the installation site.

The water supply source selected for the system is the New West well located on the Cavaletto Road at the southern edge of the Puma Canyon Ranch property. The well contains a reliable year round source of high mineral content freshwater and the borehole is 570*ft* deep as reported by the A&A Pump and Well Service of Buellton, California during their most recent service. The well borehole has an internal diameter of 6*in*. Long-term data provided by the ranch owners suggests that on average the water level in the well is approximately 126*ft* below ground level. This figure comes with a word of caution from the ranch owner who states that during summer, when the water table is low, the water level is near the bottom of the well. This indicates that any pump installed in the well must be placed at the bottom of the borehole to ensure a year-round water supply. The well site lies in a shallow canyon that runs west to east along the Puma Canyon Ranch property line and affords almost no southern exposure to the sun during morning and evening hours. There is an area of at least 20ft^2 around the well that is clear, stable and approximately level.

Due to the poor southern exposure of the well site a different location was selected for the installation of the solar array. The solar collection site is 185*ft* north of the well site on a hillside with a slope of approximately 45 degrees. The area is clear, un-shaded by trees or other obstacles and has a clear view of the horizon to the south ensuring maximum solar exposure throughout the day.

The water in the system will be pumped to the surface of the well and into an intermediate storage tank located at the well site 2ft from the surface of the well. The

tank is a 12*ft* cylindrical steel water storage tank with a diameter of 10.5*ft* and a capacity of 7500 *U.S. gallons*. The entrance to the tank is 12*ft* above ground level. From the intermediate storage tank the water is then pumped up hill to the main storage tank, which is located at the point of highest elevation on the Puma Canyon Ranch. Water from this tank can be used to supply irrigation to all of the avocado groves on the property and also to the ranch house living area.

The authors used a Garmin GPS 76 to measure the elevation gain between each station in the pumping system in order to determine the total static pressure head for the system. All of the altitude measurements were made on the same day and the GPS was calibrated at sea level before it was used to take field measurements at the ranch. The total elevation gain from the surface of the New West well to the entrance of the main storage tank is $\Delta z_{lift}=299\pm14ft$. The authors visually determined the shortest feasible distance between the New West well and the main storage tank and then used a flexible surveyor's measuring tape to measure the distance along the ground between the two points in order to determine the required pipe length. The length of pipe required to transport water from the New West well to the main storage tank is $l_{lift}=1145\pm5ft$. Figure 5 is a simplified schematic illustrating the physical dimensions of the engineering model and its major components.

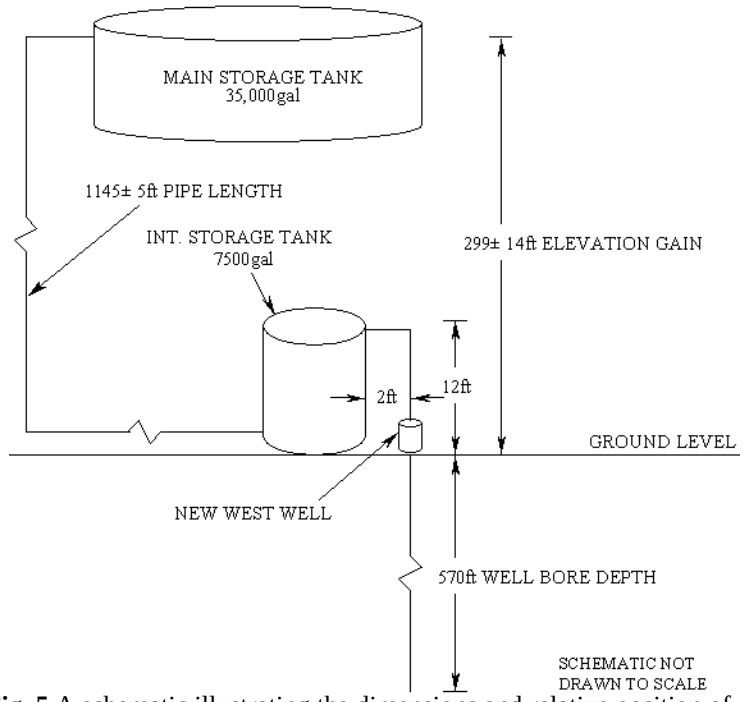

Fig. 5 A schematic illustrating the dimensions and relative position of the major components of the pumping system

System Improvement, Reliability and Longevity Concerns

In addition to the physical constrains imposed by the topography of the system's location several other environmental factors must be included in the engineering model. The first issue is the corrosion of piping materials and the long-term effects of corrosion on the entire pumping system. The existing water pumping system installed at the New West well uses galvanized steel pipe to transport water to the surface of the well and

Type I PVC pipe to transport water from surface of the well to the main storage tank. Galvanized steel piping is inadequate in this application because the interior surface of the pipe rapidly corrodes due to the high mineral content of the water supply. Over time corrosion build up on the inner walls of the pipe causes a dramatic reduction in the inner diameter of the pipe (see Figure 6) and drastically increases the total effective pumping head for the system. This increase in the total effective pumping head causes an increase in load on the pump. This extra load will cause the pump to stall and eventually result in premature failure of the pump motor.

With the existing system corrosion build up in the well drop pipe becomes severe enough to cause the pump to stall after about three to five years of service. This means that the galvanized steel drop pipe of the existing system must be completely replaced every three to five years. The cost of this maintenance schedule is unacceptable and the redesigned system will have a drop pipe with a minimum service life of 15 to 20 years.

Fig. 6 A section of heavily corroded 1" Schedule 40 galvanized steel pipe removed from the New West well in July 2007. The original diameter (approx. 1.049") outlined in green has been reduced to nearly 0.5" by corrosion buildup (red).

The New West well has been in nearly continuous service since 1989 with a period of inactivity from 1992 through 1994. The existing system pumps water from the well at an average rate of 13.9 *gallons per minute*. The New West well has a relatively slow recovery rate, and the existing pump operates on a two week on, two week off schedule for up to ten hours per day in order to avoid pumping the well dry. This complicated operating schedule requires an operator to constantly monitor the pump and the water level in the well to determine when to operate the pump. The operation of the redesigned system will be dependant on the sun and the new pump will operate only during hours of sufficient sunlight, eliminating the need for daily observation of the pump. In addition the high flow rate of the existing system and the slow recovery rate of the aging well create the potential for permanently overdrawing the existing water table and forcing early retirement of the well. The redesigned system will support a much lower flow rate then the existing system, which will help to prolong the service life of the well and allow for continuous daytime operation of the pump.

Selection and Sizing of Piping Materials

There are three major concerns regarding the selection of piping materials. The chosen pipe must meet the mechanical requirements of the system, have sufficient corrosion resistance to prevent corrosion build up and be cost effective. According to the McGraw-Hill Piping Handbook, the most desirable piping material for water pumping applications is Polyvinyl Chloride (PVC) piping due to its favorable working pressure rating and excellent chemical resistance.[16] Type I, Grade 1 drawn PVC piping material

has a yield strength of $\sigma_{ys}=8.35ksi$[17] and a roughness factor of $\varepsilon_{PVC}=0.0015\pm0.0009mm$.[18] Type I, Grade 1 drawn PVC piping will be used for all pipes above the surface of the well. For corrosive water applications where PVC is not suitable or higher strength is required 18-8 Cr-Ni piping is recommended.[19] 18-8 Cr-Ni corresponds to AISI Type 304 Stainless steel, which contains 18-20% Chromium and 8-10.5% Nickel, has a yield strength of $\sigma_{ys}=31.2ksi$[20] and a roughness factor of $\varepsilon_{SS}=0.002\pm0.001mm$.[21] In order to conserve costs Type 304 Stainless steel will be used only in the drop pipe section where reliability is critical. All the piping for the system will be $1in$ National Pipe Thread (NPT) Schedule 40, with a nominal wall thickness of $t=0.133in$, an outer diameter of $d_o=1.315in$ and an inner diameter of $d_i = 1.049in$.[22]

In order to ensure that the pipes in the system will not burst it is necessary to compute the maximum allowable pressure for each type of pipe. The maximum allowable pressure rating for each type of piping material is determined from the hoop stress experienced when each material is stressed at its respective yield strength. For thin-walled pressure vessels where the ratio of the wall thickness to the outer diameter is less than 10% Barlow's formula provides an accurate representation of the maximum allowable pressure in the pipe. Barlow's formula, which is given by,

$$\sigma = \frac{pd_o}{2t} \Rightarrow p_{\max} = \frac{2\sigma_{ys}t}{d_o} \qquad (9)$$

yields a value of p_{max} that is approximately 3% lower than the experimental failure value for thin walled pressure vessels.[23] For Schedule 40 pipe the ratio $t/d_o=0.10$, and by applying Equation 9 it is determined that $p_{max,PVC}=1.67ksi$ and $p_{max,SS}=6.24ksi$.

Computation of Total Pumping Head

With the engineering model defined and the piping materials and sizes selected it is possible to compute the total pumping head for the system. The total pumping head is defined as the sum of the static head, the friction head losses and the minor head losses in the system and is represented mathematically as,[24]

$$\Delta h_{total} = h_s + h_f + h_m = \left(z_2 - z_1\right) + \frac{V^2}{2g}\left(f\frac{L}{d} + \Sigma K\right) \qquad (10)$$

The static head ($h_{s)}$ arises due to the gravitational force that acts on the fluid in the piping system and presents the largest contribution to the total pumping head. The static head is generally taken as the height difference between the pump source inlet and the pump outlet. The friction head losses (h_f) in the system are due to the wall shear stress encountered at the interface between the fluid in the pipes and the pipe walls. At this interface a frictional force acts on the fluid opposing its motion. It is seen from Equation 10 that in general the friction head losses increase with pipe length (L) and are inversely proportional to the inner diameter of the pipe (d). Additionally the friction head losses are related to a friction factor (*f*), which is dependant on the Reynolds number (Re_d) of the flow and the relative roughness of the inner pipe walls (ε). The minor head losses (h_m) in the system arise from regions of unstable turbulent flow occurring in pipe fittings,

Pipe Fitting	Grundfos	Conergy
Sharp Entrance (K=0.5)	0	1
Sharp Exit (K=1.0)	1	1
90° Long Radius Bend (K=0.72)	1	0
45° Regular Screwed Bend (K=0.32)	0	10
Globe Valve (K=8.2)	0	2

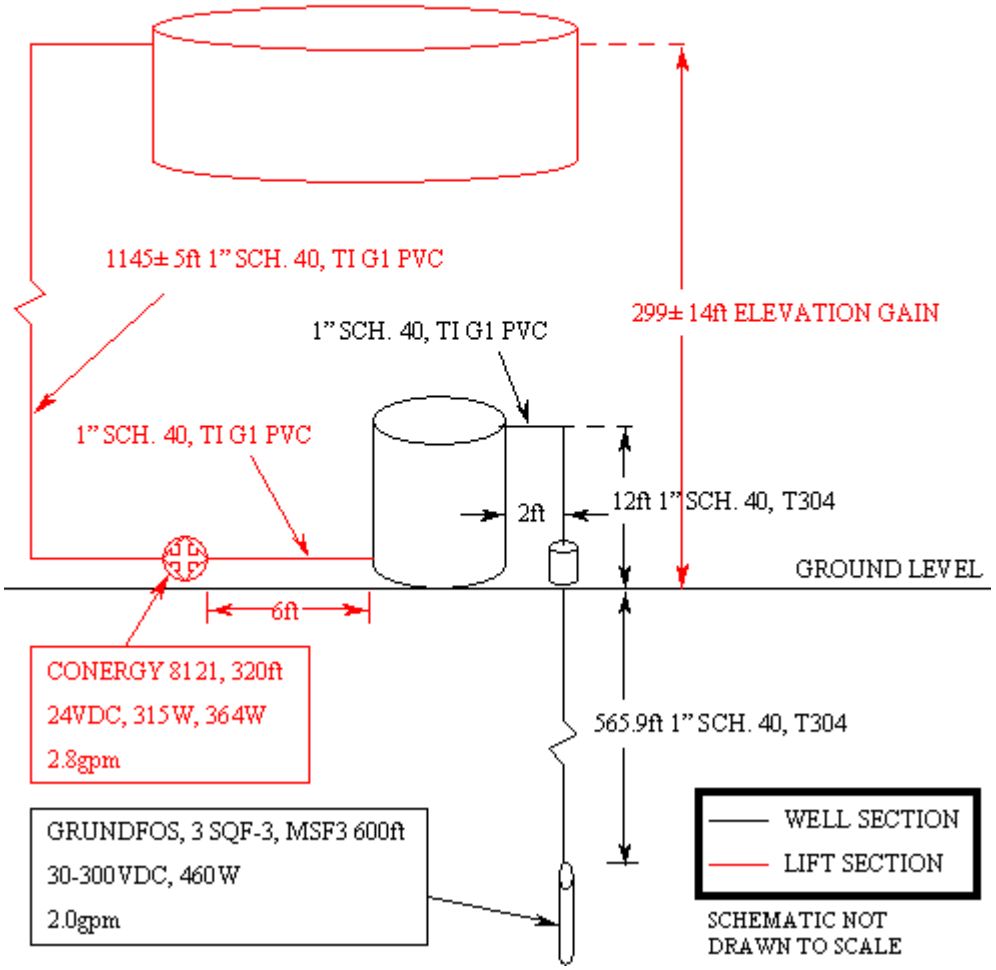

Fig. 7 A schematic illustrating the controlling pumps for each section of the system and the length and type of pipe material that will be used in each section. The table lists the type and number of pipe fittings that will be used in each section.

connectors and valves. The magnitude of the head loss contributed by these unstable flow regions is quantified by a loss factor (K), which is specific to each type of fitting and independent of the fitting material. It is important to note that while the magnitude of the minor head losses in2creases with flow velocity, the minor head losses provide the smallest contribution to Equation 10 for long pipe lengths with low flow velocities.

Figure 7 is a schematic illustration of the mechanical elements of the pumping system. The system is divided into two sections, the well section shown in black and the lift section shown in red. A submersible pump placed at the bottom of the New West well facilitates water transport from the bottom of the New West well to the intermediate storage tank near the surface of the well. A second non-submersible pump

lifts the water from the intermediate storage tank to the main storage tank. The diagram in Figure 7 shows the length and type of pipe material that will be used in each section of the system and provides a table that lists the type and number of fittings that will be used in each section.

In this analysis the fluid being pumped through the system is approximated as incompressible water (H_2O) at a pressure of 1 atmosphere and 20˚C. Assuming these conditions the density and viscosity of water are defined to be $\rho_{H2O}=998 kg/m^3$ and $\mu_{H2O}=1.00\cdot10^{-3} kg/(m\cdot s)$ respectively[25]. From these two quantities the kinematic viscosity of water is determined to be $\nu_{H2O}=1.00\cdot10^{-6} m^2/s$. Because the system is divided into two separate sections that are each powered by an independent pump, the total pumping head will be determined for each section separately.

Well Section Total Pumping Head

The static head in the well section of the system, determined directly from Figure 7, is $h_s=577.9 ft$.

The nominal volumetric flow rate of water in the well section of the system is selected to be 2.0 *gallons per minute*. In order to determine whether the flow in this section of the system is in the turbulent or laminar regime it is necessary to define the dimensionless Reynolds number with respect to the diameter of the pipe. The Reynolds number is defined as,[26]

$$\mathrm{Re}_d = \frac{Vd}{\nu} = \frac{Qd}{A\nu} \qquad (11)$$

Using this definition it is determined that the Reynolds number for the internal flow in the well section of the system is $\mathrm{Re}_d=6030$. For internal pipe flow, the laminar to turbulent transition occurs when $\mathrm{Re}_{d,cr}\approx2300$.[27] This transitional value indicates that the flow in the well section of the system is in the turbulent regime.

Based on the determination that the flow in the well section is turbulent the friction factor for each type of pipe material can be computed by numerically evaluating the Colebrook equation for the friction factor. The Colebrook equation is given by,[28]

$$f^{-0.5} = -2.0\log\left(\frac{\varepsilon/d}{3.7} + \frac{2.51}{\mathrm{Re}_d\, f^{0.5}}\right) \qquad (12)$$

The friction factor for 1” Nominal, Schedule 40, Type I, Grade 1, PVC pipe determined by numerically iterating* Equation 12 is $f_{PVC}=0.03556$. The friction factor for 1” Nominal, Schedule 40, T304 stainless steel pipe determined by numerically iterating Equation 12 is $f_{SS}=0.03559$. For both values of the friction factor a maximum value for the parameter ε has been assumed in order to avoid choosing a pump that is too small during subsequent analysis.

The total pumping head for the well section of the system can be determined by evaluating Equation 10 using these values for the friction factor and the dimensions and

* Equation 12 was evaluated numerically for *f* using the Equation Solver program of a Texas Instruments TI-86 calculator.

loss coefficients from Figure 7 as well as the previously computed value for the static head in the well section. The total pumping head for the well section is Δh_{total}=598.1*ft*. This value represents the total head that must be supplied by the submersible pump in the New West well to fill the intermediate reservoir at a rate of 2*gpm*.

Lift Section Total Pumping Head

The static head in the lift section of the system, determined directly from Figure 7, is h_s=299±14*ft*. This analysis will assume a maximum value for the static head of h_s=313*ft* in order to avoid choosing a pump that is too small during subsequent analysis.

The nominal volumetric flow rate of water in the lift section of the system is selected to be 2.8 *gallons per minute*. Using this value and Equation 11, the Reynolds number for the lift section flow is determined to be Re_d=8440 which is greater than the critical value indicating that the lift section flow is in the turbulent regime. Equation 12 can be solved for 1" Nominal, Schedule 40, Type I, Grade 1, PVC pipe in the lift section to determine *f*=0.03556.

The total pumping head for the lift section of the system determined using Equation 10 is Δh_{total}=327.3*ft*. This value represents the total head that the lift pump must supply in order to raise water from the intermediate storage tank to the main storage tank at a rate of 2.8*gpm*.

Pump Selection and Power Requirements of Pumps

There are a number of different companies that manufacture a variety of models of DC solar water pumps and for this application two different types of pumps were selected from different manufacturers.

A Grundfos 3 SQF-3 submersible helical rotor type pump powered by a Grundfos MSF 3 submersible permanent magnet DC motor was selected for the well section of the system.[*] The pump and motor are separate units and are bolted together at the motor drive axle interface forming the complete pump assembly. The motor transfers power to the pump through a splined driveshaft. The pump assembly has an expected service lifetime of 20 years when the pump is operated under ideal conditions. The complete pump assembly is cylindrical in shape and requires a minimum well borehole diameter of 3*in*. The pump may be safely installed up to 500*ft* below the static water table where the ambient hydrostatic gauge pressure of 220*psi*. The pump motor has several built-in redundancy systems that protect the motor against dry running, overvoltage and undervoltage power supply, motor overload conditions and motor overtemperature conditions.

The pump motor may be powered using a DC or an AC power supply. In this application the motor is powered directly from the solar array and will operate in DC mode. In DC mode the pump operates in an input voltage range of 30-300*VDC* with a maximum power input of 900*W* and maximum current input of 8.4*A*.

The complete pump assembly will be installed at a maximum depth of 444*ft* below the static water table where the hydrostatic gauge pressure is 192*psi*. Based on the performance curves for the 3 SQF-3 the complete pump assembly requires 460*W* to support a total pumping head of 598*ft* at a flow rate of 2.0*gpm*.

[*] For a complete list of specifications and the performance curves for the Grundfos 3 SQF-3 and the MSF 3 see Appendix A.

A Conergy Solaram Surface Pump Model Number 8121 was selected for the lift section of the system.* The Conergy 8121 is a multiple-diaphragm positive displacement pump, which is powered by a permanent magnet 24*VDC* motor. The motor and the pump are mounted together on cast aluminum casing and the motor transfers power the pump through a positive transfer timing belt. The pump assembly is not submersible and must be installed in a dry, protected location. When operated under ideal conditions the complete pump assembly has a 20-year service life expectancy. In addition the Conergy 8121 may be safely operated under a dry run condition and can tolerate sediment and other small particles suspended in the water.

The Conergy 8121 requires 320*W* to support a total pumping head of 327*ft* at a flow rate of 2.7*gpm*. This power value is based on a linear interpolation of the data from the performance tables for the pump.

Electrical Design

The number and size of solar panels that will be used to power the water pumping system is dependant on the power requirements of the system's mechanical components and how the solar array is coupled to the system. In order to reduce the installation and maintenance costs of the system and to minimize the system's environmental impact, batteries will not be used to store the energy collected by the solar array. Instead the

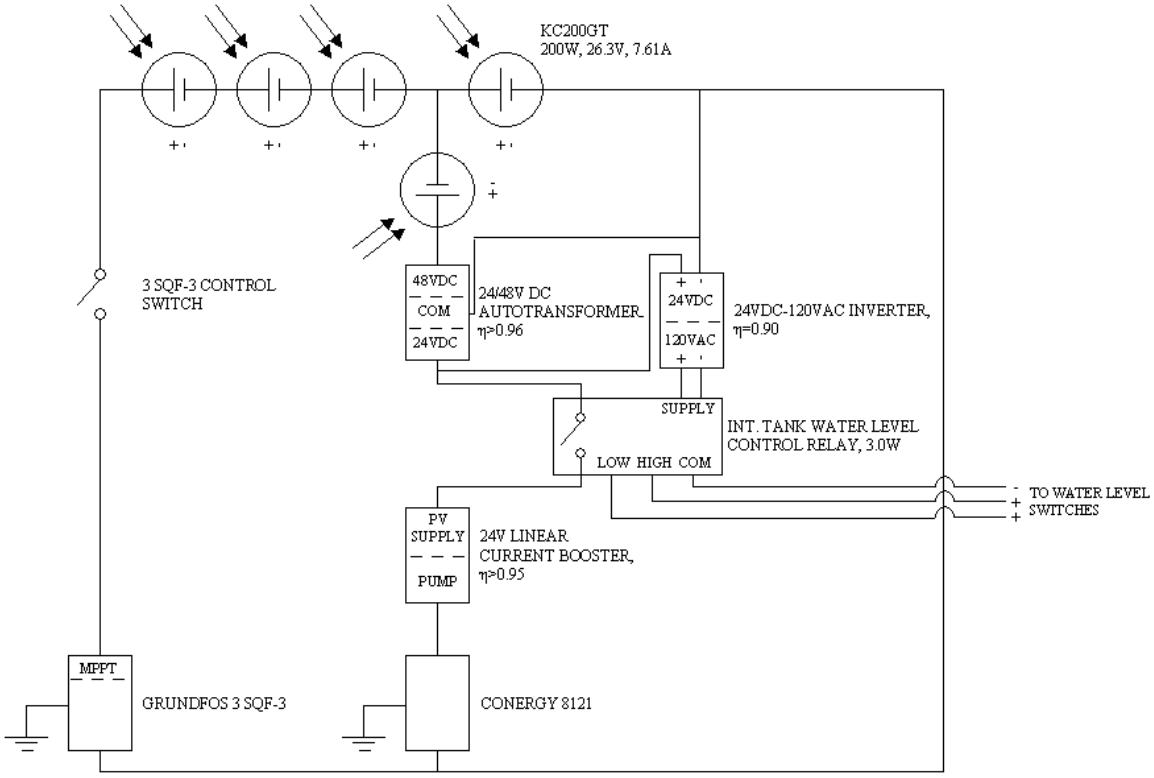

Fig. 8 A schematic illustrating the configuration of the main components in the electrical system.

* For a complete list of specifications and the performance tables for the Conergy 8121 see Appendix A.

solar array will be directly coupled to the pumps and both pumps will operate continuously during the period when the output from solar array is sufficient to support hydraulic flow in the system. Solar direct power to the pumps has the additional advantage of minimizing the amount of time an operator must spend to keep the system running. With solar direct power the pumps do not need to be switched on and off manually and will operate automatically when the sun provides enough energy.

Selection of Photovoltaic Modules

The total power required to lift water from the New West well to the main storage tank is 780*W*, with 460*W* consumed by the Grundfos pump and 320*W* consumed by the Conergy pump. Because the solar array is directly connected to the load the optimum power output of the array should exceed the power requirements of the system by approximately 25%, in order to improve the low light performance of the pumps and to account for power losses in the electrical system. The minimum power output of the solar array using a factor of safety of 125% is 975*W*. Based on these power requirements the solar array will consist of five Kyocera KC200GT modules. The KC200GT modules have a nominal maximum power output of 200*W* at a voltage of 26.3*V* and a current of 7.61*A*.[*] The KC200GT modules have a minimum service lifetime of 20 years.

Figure 8 illustrates a simplified circuit diagram of the electrical system that powers the pumps. The circuit consists of two main branches, one branch powers the Grundfos pump and the other powers the Conergy pump. Generally the system operates under one of two conditions depending on the position of the intermediate tank water level control relay. When the solar array is operating at maximum output and the level switch is open, the Conergy branch of the circuit is disconnected and the Grundfos branch draws 800*W* at 105.2*V* from four panels connected in series. When the level switch is closed the Conergy pump lifts water from the intermediate storage tank to the main storage tank. Under this condition the Conergy pump draws 400*W* at 52.6*V* and the Grundfos pump uses the remaining 600*W* at 78.9*V*. The arrangement of the circuit allows for the simultaneous operation of both pumps and when the Conergy pump is not operating the Grundfos pump draws more power from the solar array and operates with improved performance.

Optimum Angle of Solar Modules

The output of solar modules depends on their orientation and relative angle of tilt. In order to maximize the output of a solar module the panel should always face due south. The optimum angle of tilt varies seasonally and the angle of tilt from horizontal during each season is given by the following set of formulas,

Winter: (0.9)(Latitude-Decimal Degrees) + 29˚
Summer: (Winter Angle) – 52.5˚
Spring/Autumn: (Latitude-Decimal Degrees) – 2.5˚

The seasons are defined by the following dates,

[*] For a complete list of the specifications and performance curves for the Kyocera KC200GT solar module see Appendix A.

Winter: October 13th to February 27th
Spring: February 27th to April 20th
Summer: April 20th to August 22nd
Autumn: August 22nd to October 13th

Based on these formulas for optimum orientation, the solar array should be adjusted four times during the year such that the angle between the individual modules and the horizontal is 60˚ during winter, 8˚ during summer, and 32˚ during spring and autumn.[29]

Power Loss in Transmission Wires

The solar array produces power that is driven by a DC voltage at a relatively high current. Because the array is located at a distance from the load some voltage drop is experienced due to resistance in the transmission wires. The power dissipated by a resistor is given by the relation,

$$P_{loss} = I^2 R \qquad (13)$$

where I is the current through the resistor and R is the resistance.[30] In general the resistance of a cylindrical conductor increases with length and decreases as the diameter of the conductor increases. The resistance of a length of wire depends on these two properties and also on the material that the wire is made of. In this application Medium hard-drawn solid copper wire will be used to transmit power from the solar array to each pump.

The length of wire required to complete a circuit between the solar array and the Grundfos pump is 1060*ft*. The transmission wire for the Grundfos pump is size AWG 1 which has a resistance of 0.1282 ohms per 1000 feet of wire length.[31] The total resistance of the Grundfos transmission wire is 0.1935Ω and the power loss through the wire by Equation 13 is 11.2*W* corresponding to a voltage drop of 1.5*V*. When the Grundfos pump operates by itself it will receive 788.8*W* at 103.7*V*. When both pumps operate simultaneously the Grundfos pump will receive 588.8*W* at 77.4*V*.

The length of wire required to complete a circuit between the solar array and the Conergy pump is 370*ft* and the wire size is AWG 11 that has a resistance of 1.303 ohms per 1000 feet of wire length.[32] The total resistance of the Conergy transmission wire is 0.4817Ω and the power loss through the wire by Equation 13 is 27.9*W* corresponding to a voltage drop of 3.7*V*. When the both pumps operate simultaneously the Conergy pump will receive 372.1*W* at 48.9*V* before the power electronics as illustrated in Figure 8.

Power Electronics

The electrical system uses a number of power electronics that optimize the electric power distribution or duty point of each pump to match the maximum power point of the solar modules. The components in this section refer to those illustrated in Figure 8.

The internal circuitry of MSF 3 motor in the Grundfos pump assembly incorporates a built-in Maximum Power Point Tracking (MPPT) circuit that operates only when the motor is powered with a DC power supply. The MPPT circuit continuously optimizes the pump duty point in order to draw the maximum amount of power from the solar array. The MPPT circuit improves pump performance by increasing the hydraulic

flow rate in low light conditions and helps facilitate starting when the current supplied by the solar array is low.

The electrical system has two power conversion circuits placed before the Conergy pump that help to optimize the pump performance. Because the Conergy pump motor operates on 24*VDC* a DC autotransformer is used to step down the voltage supplied by the solar array from 48.9*V* to 24*V*. The DC autotransformer used in this circuit is manufactured by Solar Converters Inc. (Model No. EQ 24/48-30) and works as either an up or down converter between 24*VDC* and 48*VDC*.[*] When the autotransformer is connected in a down converter configuration the output is current limited at 30*A* and the power transformation occurs with a minimum efficiency of 96%.

The intermediate tank water level control relay requires an input voltage of 120*VAC*. A 24*VDC* to 120*VAC* inverter is connected across the DC autotransformer and the photovoltaic array and has an efficiency of 90%. The output from the inverter is the input voltage source for the water level control relay, which has a maximum power consumption of 3.3W.

The technical data for the Conergy pump specify that when the pump is connected directly to the solar array a linear current booster pump controller must be used in order to facilitate starting and prevent stalling in low light conditions. In this application a Solar Converters Inc. Model Number PPT 12/24-30 30*A* current limited linear current booster is used as the pump controller.[†] The linear current booster has a minimum efficiency of 95%.

Based on the minimum efficiency ratings of the DC Autotransformer and the linear current booster the final power available to the Conergy pump is 330*W* when the solar array is operating at maximum output. The voltage and current distribution of the power supplied to the Conergy pump is variable and automatically optimized by the linear current booster.

Intermediate Storage Tank Water Level Control

The water level in the intermediate storage tank is controlled by the operation of the Conergy pump, which is regulated by a liquid level control switch. The liquid level control switch consists of three main components, a high level switch, a low level switch and a liquid level control relay. The high and low level switches are stainless steel, mechanically actuated 70*W* single-pole single-throw Reed switches manufactured by Innovative Components (Model No. SM-1000-SS) and pressure rated to 500*psi*.[‡] The switches are mounted horizontally on the side of the intermediate storage tank in ½" NPT tapped holes. The high level switch is mounted 10" below the maximum tank water level in order to prevent tank overflow. The low level switch is mounted 6" above the tank outlet in order to protect the pump from dry running. The high and low switches share a common ground and are wired to the terminals on the liquid level control relay (see Figure 8).

The liquid level control relay is a single-pole double-throw (1 Form C) relay that controls 24*V* up to 10*A*.[§] The relay takes a source voltage of 120*VAC* and consumes a

[*] For a complete list of the specifications for the EQ 24/48-30 see Appendix A.
[†] For a complete list of the specifications for the PPT 12/24-30 see Appendix A.
[‡] For a complete list of the specifications for the SM-1000-SS Reed switch see Appendix A
[§] For a complete list of the specification for the R-DLC-120 relay see Appendix A.

maximum of 3*W*. The relay controls the operation of the Conergy pump by detecting the position of the level switches. When the water level in the tank reaches the full condition, the high level switch is tripped and the liquid level relay energizes the Conergy pump. When the level in the tank reaches the empty condition, the low level switch is tripped and the liquid level relay de-energizes the Conergy pump. The liquid level control relay is also manufactured by Innovative Components and its model number is R-DLC-120.

The R-DLC-120 relay is powered by a 24*VDC* to 120*VAC* power inverter, which is connected in the Conergy branch of the electrical system just after the DC autotransformer (see Figure 8). The inverter is manufactured by Power Inverters and the complete list of specifications can be found in Appendix A.

System Performance

Month	Estimated Daily Production (gal)	Estimated Monthly Production (gal)
January	360	1080
February	432	1555
March	588	2881
April	672	3763
May	780	5070
June	768	4915
July	780	5070
August	756	4763
September	636	3371
October	492	2017
Novermber	384	1229
December	336	941
	Total Yearly Production (gal)	36655
	Projected System Lifetime Produciton (gal)	733104

Table 2 Estimated system production.

The complete pumping system has been designed for long-term reliability with the goal of a minimum service lifetime of 15 years. Many of the actual components selected for the design exceed this minimum requirement and the overall projected service lifetime of the system is 20 years.

The system pumps water from the New West well at a rate of 2.0*gpm*. Based on this flow rate and the values for daily peak sun hours from Table 1 it is possible to make a rough estimate of how much water will be pumped by the system during one year while operating under ideal conditions. Table 2 lists the daily production of the system during each month as well as the monthly and yearly production of the system. The projected system lifetime production is based on an expected service lifetime of 20 years.

Cost Analysis

In order to determine the economic viability of the system it is necessary to perform an itemized cost analysis of the total system cost, and make estimate of the yearly and monthly cost of the system based on it projected service lifetime. A summary of the cost of each individual system component and the total cost of all components is presented in Table 1B of Appendix B. The total estimated cost for the installed system $14,941.96. Based on an estimated service lifetime of 20 years the estimated yearly cost of the system is $747.10 and the estimated monthly cost of the system is $62.26. Based on the projected system lifetime production the equivalent cost of water is $0.02 per gallon.

It is also necessary to complete a comparative cost analysis in order to determine how costs of the photovoltaic pumping system compare to current water rates posted by the Goleta Water District, the controlling water agency in the vicinity of the Puma Canyon Ranch. For agricultural irrigation customers with a standard 1" water meter, the Goleta Water District currently charges a monthly meter charge of $46.06 and an additional volume charge of $1.00 per hundred cubic feet (HCF).[33] Table 2B in Appendix B lists the equivalent system cost if the same amount of water produced by system were purchased from the Goleta Water District. From Table 2B the yearly cost increase of the photovoltaic system versus the equivalent cost of public water is $145.38. It is important to note, however, that the Goleta Water District does not currently supply water to the Puma Canyon Ranch, and the added cost of running water mains to the property would likely offset this yearly cost increase.

Conclusions and Application Extensions

Based on the results of the cost analysis high performance photovoltaic deep-well water pumping systems do not provide an affordable solution for small-scale agricultural applications where profit margins are narrow. While the cost increase of the photovoltaic system is not prohibitively large, the volume of water pumped by the system is not great enough to keep up with the large volume demands of a working farm. Increasing the flow rate of the system would cause a disproportionately large increase in the overall system cost and the cost per gallon of water pumped. The system could be applied in a more cost effective manner to small farm applications where the total system head is much lower, and the power requirements of the pumps is greatly reduced.
Although the system is not a viable solution in the agricultural sector where high volumes water are required, there are a number of other applications in which a deep-well, low-flow photovoltaic pumping system similar to the one of this report would prove applicable. One such application is providing water for an off-grid home site that is located a long distance from public water and electricity grids, where the cost of plumbing water mains and running grid power to the property is so great that it becomes prohibitive to home construction. In such an instance the system would provide an ample supply of water for regular domestic use. In addition deep-well pumping systems provide a sustainable solution for supplying rural communities with water, especially in areas arid regions where the water table is located far below ground level. Similar systems could also be implemented in high fire risk, backcountry areas to aid in the prevention of wild fires that could be potentially damaging to homes and other structures.

Sources

[1] Komp, Richard J. Practical Photovoltaics Electricity From Solar Cells. aatec: Ann Arbor. 1995 (Pg. 5)

[2] Messenger, Roger A. and Jerry Ventre. Photovoltaic Systems Engineering, Second Edition. CRC Press: Boca Raton. 2003 (Pg. 55)

[3] Messenger, Ventre (Pg. 54)

[4] Messenger, Ventre (Pg. 22)

[5] Meinel, A . B . and Meinel, M . P ., *Applied Solar Energy, an Introduction,* Addison-Wesley, Reading, MA, 1976

[6] Messenger, Ventre (Pg. 29, Eq. 2.7)

[7] Komp (Pg. 5)

[8] Messenger, Ventre (Pg. 30, Eq. 2.11)

[9] Messenger, Ventre (Pg. 26, Eq. 2.5)

[10] Messenger, Ventre (Pg. 29, Eq. 2.8)

[11] Messenger, Ventre (Pg. 30, Eq. 2.9)

[12] California Information Management System. "Station Detail Report, Goleta Foothills #94" April 19th, 2008. <http://wwwcimis.water.ca.gov/cimis/frontStationDetailData.do?stationId=94>

[13] California Information Management System. "Sensor Specs, 1. Total Solar Radiation (pyranometer)" April 19th, 2008. <http://wwwcimis.water.ca.gov/cimis/infoStnSensorSpec.jsp>

[14] California Climate Data Archive. "Goleta Foothills California" April 19th, 2008. <http://www.wrcc.dri.edu/cgi-bin/rawMAIN.pl?caZGOF>

[15] Messenger, Ventre (Pg. 25)

[16] King, Reno C. Piping Handbook. McGraw-Hill: New York. 1967 (Pg. 7-293)

[17] MatWeb Material Property Data. "Quadrant EPP PVC – Polyvinyl Chloride, Type I, Grade 1" May 25th, 2008. < http://www.matweb.com/search/DataSheet.aspx?MatID=20184>

[18] White, Frank M. Fluid Mechanics, Sixth Edition. McGraw-Hill: New York. 2008 (Pg. 365)

[19] King (Pg. 9-21)

[20] MatWeb Material Property Data. "304 Stainless Steel" May 25th, 2008. <http://www.matweb.com/search/DataSheet.aspx?MatID=12674&ckck=1>

[21] White (Pg. 365)

[22] King (Pg. 7-20)

[23] King (Pg. 3-15)

[24] White (Pg. 383, Eq. 6.79)

[25] White (Pg. 817)

[26] White (Pg. 27)

[27] White (Pg. 346, Eq. 6.2)

[28] White (Pg. 363, Eq. 6.48)

[29] Landau, Charles R. "Optimum Orientation of Solar Panels". June 9th, 2008. <http://www.macslab.com/optsolar.html>

[30] Wolfson, Richard, Jay M. Pasachoff. Physics for Scientists and Engineers. Pearson Addison Wesley: Boston. 1999 (Pg. 701, Eq. 27-9a)

[31] Croft, Terrell, Wilford I. Summers. American Electrician's Handbook, 14th Edition. McGraw-Hill: New York. 2002 (Pg. 2.47)

[32] Croft, Summers (Pg. 2.47)

[33] Goleta Water District. "Rates, Bills & Budget". June 9th, 2008. <http://www.goletawater.com/rates/index.htm>